Citation: Molecular Therapy — Methods & Clinical Development (2016) **5,** 16066; doi:10.1038/mtm.2016.66
Official journal of the American Society of Gene & Cell Therapy

www.nature.com/mtm

ARTICLE

The feasibility of incorporating Vpx into lentiviral gene therapy vectors

Samantha A McAllery[1], Chantelle L Ahlenstiel[1], Kazuo Suzuki[2], Geoff P Symonds[2,3], Anthony D Kelleher[1,2] and Stuart G Turville[1]

While current antiretroviral therapy has significantly improved, challenges still remain in life-long targeting of HIV-1 reservoirs. Lentiviral gene therapy has the potential to deliver protective genes into the HIV-1 reservoir. However, inefficient reverse transcription (RT) occurs in HIV-1 reservoirs during lentiviral gene delivery. The viral protein Vpx is capable of increasing lentiviral RT by antagonizing the restriction factor SAMHD1. Incorporating Vpx into lentiviral vectors could substantially increase gene delivery into the HIV-1 reservoir. The feasibility of this Vpx approach was tested in resting cell models utilizing macrophages and dendritic cells. Our results showed Vpx exposure led to increased permissiveness of cells over a period that exceeded 2 weeks. Consequently, significant lower potency of HIV-1 antiretrovirals inhibiting RT and integration was observed. When Vpx was incorporated with anti-HIV-1 genes inhibiting either pre-RT or post-RT stages of the viral life-cycle, transduction levels significantly increased. However, a stronger antiviral effect was only observed with constructs that inhibit pre-RT stages of the viral life cycle. In conclusion this study demonstrates a way to overcome the major delivery obstacle of gene delivery into HIV-1 reservoir cell types. Importantly, incorporating Vpx with pre-RT anti-HIV-1 genes, demonstrated the greatest protection against HIV-1 infection.

Molecular Therapy — Methods & Clinical Development (2016) **5**, 16066; doi:10.1038/mtm.2016.66; published online 19 October 2016

INTRODUCTION

Current drug therapy has greatly improved prognosis for HIV-1 infected patients, reducing HIV-1 RNA in the blood to almost undetectable levels (<50 copies/ml).[1–3] However HIV-1 persists in cellular reservoirs of certain long-lived immune cells, including quiescent CD4+ T cells (qCD4+ T cells), dendritic cells and monocytes/macrophages.[4–7] Consequently, upon cessation of treatment HIV-1 levels rapidly rebound.[8,9] It has been estimated that the half life of qCD4+ T cells is 44 months and has been projected to take up to 60 years of continuous drug therapy to clear HIV-1 from this one latent reservoir.[5,10–12] Alternative approaches are needed, resulting in a HIV-1 functional cure outside of recurrent combination antiretroviral therapy.

Targeting the HIV-1 latent reservoir and/or protection of future HIV-1 target cells is a crucial step toward a HIV-1 cure. One method of achieving this is through gene therapy. Multiple approaches have been used inhibit HIV-1 infection, which include inhibiting CCR5 expression through zinc finger nucleases,[13,14] hammerhead ribozymes[15,16] and RNA interference.[17–20] Additionally, the potential for permanently silencing the latent HIV-1 reservoir has been demonstrated through transcriptional gene silencing in the HIV-1 promoter region.[21–23] While there are diverse approaches in tackling the latent reservoir, efficient delivery with current lentiviral (LV) gene therapy vectors is limited. This lack of delivery is due to inefficient RT of genetic constructs, resulting in poor integration and gene expression.[24]

A cellular protein, SAMHD1, has been established as the HIV-1 restriction factor responsible for inefficient gene delivery in resting cells, such as the latent HIV-1 reservoir.[25,26] SAMHD1 was first discovered to hydrolyse the cellular deoxynucleotides (dNTP) pool to a point below the threshold required for efficient RT.[27,28] Recently, it has also been discovered to exhibit RNAse activity that degrades HIV-1 RNA.[29–31] Nonetheless, both of these effects are relevant to HIV-1 and LV gene therapy vectors, as both carry RNA genetic information and utilize HIV-1 reverse transcriptase before genetic integration within the host genome.

For successful gene delivery into the latent HIV-1 reservoir, efficient RT needs to occur for integration and subsequent gene expression. A viral protein called Vpx, encoded by the Sooty Mangabey SIV (SIV_{SM}) and HIV-2 lineages has been shown to alleviate SAMHD1 mediated HIV-1 restriction.[25,26] Experiments have revealed that Vpx degrades SAMHD1 through the proteasomal dependent degradation pathway.[32–34] In the absence of SAMHD1, the cellular dNTP levels can increase above the threshold needed for efficient LV RT.[35] This phenotype supports the future use of Vpx in the context of LV gene therapy vectors and DC-based vaccines.[26,36–39]

While this has immense potential in gene therapy strategies for an HIV-1 cure, the effects of introducing Vpx into an HIV-1 positive individual *in vivo/ex vivo* are not known. This needs to be carefully considered since the positive effect Vpx has on RT for lentiviral gene therapy vectors would also affect existing HIV-1 infected cells. To determine the feasibility of Vpx being incorporated into

[1]The Kirby Institute, University of New South Wales, Sydney, Australia; [2]St Vincent's Center for Applied Medical Research, Darlinghurst, Australia; [3]Calimmune Pty Ltd., Darlinghurst, Australia. Correspondence: SG Turville (sturville@kirby.unsw.edu.au)
Received 19 August 2016; accepted 31 August 2016

lentiviral gene therapy vectors, this study sought to characterize three unknowns in utilizing Vpx. Firstly, if cells were exposed to Vpx *ex vivo*, do the effects of Vpx rapidly decay? Secondly, does Vpx affect the efficacy of antiretroviral therapy, and if so, how long post-Vpx exposure does this persist? Finally, since Vpx increases viral RT would there be differences in HIV-1 protection if Vpx was incorporated with anti-HIV-1 genes that inhibited HIV-1 infection pre- or post-RT? To investigate these key questions an important resting cell type model of monocyte derived macrophages (MDMs) generated from primary cells was used.

RESULTS

Vpx uncouples and increases the kinetics for the process of reverse transcription and integration in macrophages

We used macrophages as the resting cell model in the following experiments as they express high levels of SAMHD1 and contain a depleted cellular dNTP pool, which is common to all cells of the latent HIV-1 reservoir. To address whether Vpx would make a suitable candidate to incorporate into gene therapy vectors, we first performed a time of addition assay. By assessing the effect Vpx has on RT and integration, the kinetics of short-term Vpx exposure could be mapped (Figure 1a). The length of time taken for the antiretrovirals to lose their antiviral activity was interpreted as the completion of the part in the HIV-1 replication cycle that the drug inhibits. Therefore, azidothymidine (AZT) and raltegravir (RAL) were used to determine the RT and integration kinetics, respectively. As HIV-1 and HIV-1 based lentiviral vectors share the same reverse transcription and integration pathway, we initially used a replication incompetent HIV-1 clone that expressed green fluorescent protein (GFP) as a simple surrogate to map kinetics of RT and integration.

Analysis of the AZT/RAL time of addition assay in Figure 1b revealed that the control virus (HIV-1 GFP-Vpx) had comparable kinetics for both RT and integration with their 50% completion of HIV-1 infection occurring within 1 hour from each other (AZT –Vpx = 26.78 hpi and RAL –Vpx = 25.74 hpi). Whereas, upon Vpx exposure the RT and integration kinetics increased and separated with the 50% completion of HIV-1 infection from AZT and RAL treated cells occurring 17.63 and 9.47 hours earlier, respectively (AZT + Vpx = 9.15 hpi and RAL + Vpx = 16.37 hpi). Interestingly, the separation of RT and integration kinetics observed upon Vpx exposure is also observed in other cell types with abundant cellular dNTP pools,[40] such as the HeLa cell line TZMbl (Supplementary Figure S2).

The increase in kinetics does not take into account the magnitude of completed RT and integration events. Since GFP expression is indicative of successful integration and gene expression we compared the total number of GFP positive cells between replication incompetent HIV-1 GFP packaged with and without Vpx to evaluate the effect on successful gene delivery. In the presence of Vpx a significantly higher number of GFP expressing macrophages were observed from 6 hpi and 18 hpi in the AZT and RAL treated cells, respectively ($P < 0.0001$) (Figure 1c). Therefore, Vpx not only increases RT and integration kinetics, but also increases the overall magnitude of HIV-1 infection. Previous studies have also confirmed the enhancement of HIV-1 infection post Vpx exposure.[36,41]

Vpx enhances HIV-1 infection long term in macrophages

To determine any potential deleterious effects, which could occur in the *in vivo* HIV-1 reservoir post-Vpx stimulation, the period cells retained enhancement to HIV-1 infection after Vpx exposure was investigated. To address this question the experimental design was modeled to a typical *ex vivo* gene therapy protocol.[42] As a Vpx protein delivery platform, we generated VSVg pseudotyped virus-like particles (VLPs). The VLPs are identical to lentiviral vectors, yet package Vpx protein and lack vector RNA. Briefly, macrophages were spinoculated with VLPs packaged with or without Vpx (VLPs ± Vpx). We then determined the period post-Vpx exposure with which primary cells would be vulnerable to Vpx enhanced infection. At multiple time points poststimulation, the cells were challenged with a replication incompetent HIV-1 GFP. The infection time points represented the time at which the *ex vivo* transduced cells were transferred back into an HIV-1 positive patient (Figure 2). The level of enhanced HIV-1 infection and SAMHD1 protein levels were determined for each time point.

When macrophages were stimulated with Vpx containing VLPs, enhancement of HIV-1 infection was observed across all donors to at least 14 days poststimulation (dps) (Figure 3a,b). The protein level of SAMHD1 in macrophages remained low during the time course, with levels only starting to increase at 14 dps (Figure 3c and Supplementary Figure S3a). The observed long-term enhancement of HIV-1 infection upon Vpx stimulation raises questions of the suitability of Vpx to be incorporated into gene therapy vectors. However, this data is only from one resting cell type. We sought to gather more evidence using other cell types to determine whether this was just a macrophage specific effect.

Vpx enhances HIV-1 infection long term in dendritic cells

We turned our attention to another cell type, monocyte derived dendritic cells (MDDCs). These cells are also sensitive to Vpx, making them suitable to further investigate our above observations. The same experimental protocol outlined for macrophages was also used for MDDCs. Upon analysis a comparable trend was observed from 1 dps onwards (Figure 3d,e), with enhancement of HIV-1 infection observed across all donors to at least 14 dps. The SAMHD1 protein expression pattern for MDDCs showed complete degradation by 5 dps. This level remained stable for the length of the experimental time course, which was a contrast to macrophages, which only had partially depleted levels of SAMHD1 (Figure 3f and Supplementary Figure S3b).

Vpx affects the efficiency of AZT, EFV, and RAL both short and long term

Previous studies have shown Vpx stimulation causes a significant decrease in HIV-1 sensitivity to various nucleoside reverse transcription inhibitors.[43,44] We examined whether Vpx could alter the efficiency of AZT and RAL, for both short and long-term time points post-Vpx stimulation. Log dose-response curves were generated to compare relative drug efficiencies at 1 and 7 dps. Upon Vpx stimulation macrophages showed a considerable reduction of sensitivity to AZT at both 1 and 7 dps (Figure 4a), while sensitivity to Efavirenz (EFV) and RAL was also reduced, but to a lesser extent (Figure 4b,c). From the log dose-response curves the IC_{50} were calculated. Upon analysis the AZT IC_{50} values from both time points were significantly different between –Vpx and +Vpx stimulated samples ($P < 0.05$; $n = 4$) (Figure 4d), with the difference median values of 1 and 7 dps being –3.11 and –0.36 µmol/l, respectively. The EFV IC_{50} values were not significantly different between –Vpx and +Vpx stimulated samples (Figure 4e). The RAL IC_{50} values for 1 dps was significantly different between –Vpx and +Vpx stimulated samples ($P < 0.05$; $n = 4$) (Figure 4f), with the difference median values of 1 dps being –0.02 µmol/l. The

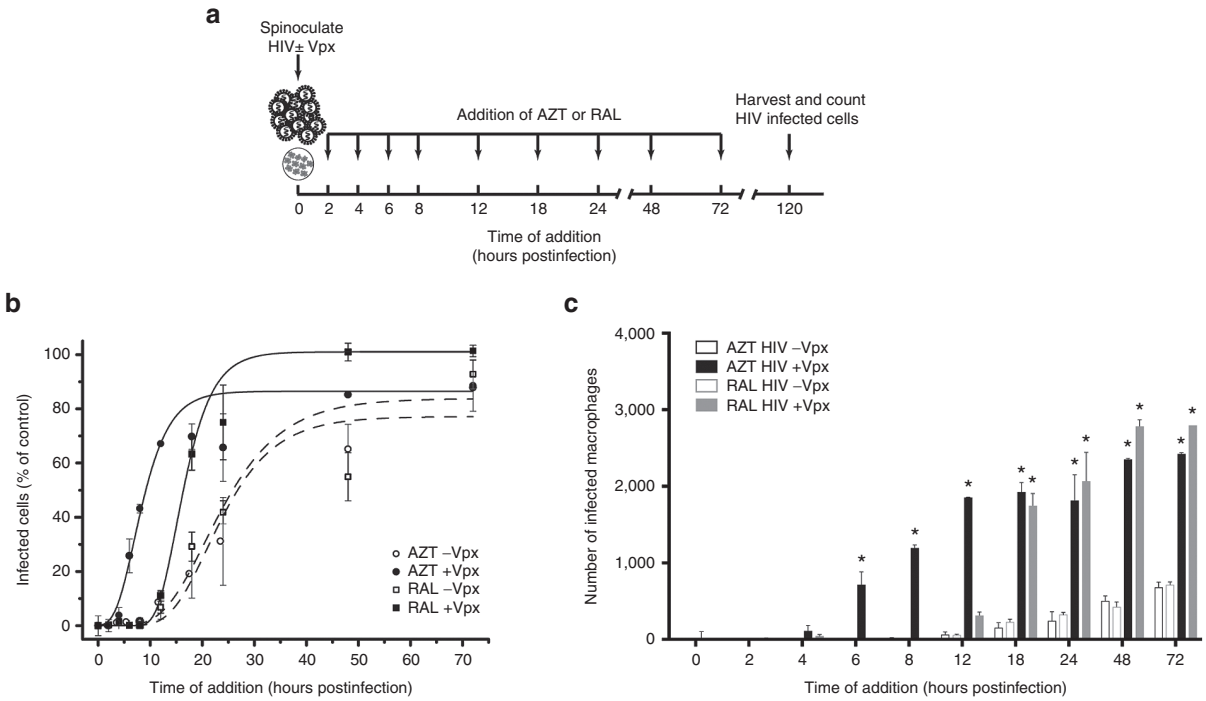

Figure 1 The short-term effect of Vpx on lentiviral reverse transcription and integration. (**a**) Protocol outline of AZT/RAL time-of-addition assay. (**b**) Reverse transcription and integration kinetics of HIV-1 GFP packaged with or without Vpx, protocol outlined in **a**. After spinoculation of MDM with HIV-1 GFP packaged with or without Vpx, the antiretrovirals were added at indicated time points, spanning from 0–72 hours post- infection (hpi). AZT (10 µmol/l) was used as a surrogate for reverse transcription and RAL (1 µmol/l) was for use for integration. Lentivirus infected cells were enumerated by GFP fluorescence at 120 hpi. Relative infection (%) compared with the noninhibited replication control is plotted. Each data set was fitted with a sigmoidal curve. (**c**) Total number of GFP positive cells for each data point outlined in Figure 1b. Mean + SD were plotted; $n = 3$. One representative MDM donor of three is displayed. AZT, azidothymidine; MDM, monocyte derived macrophage; GFP, green fluorescent protein; SD, standard deviation.

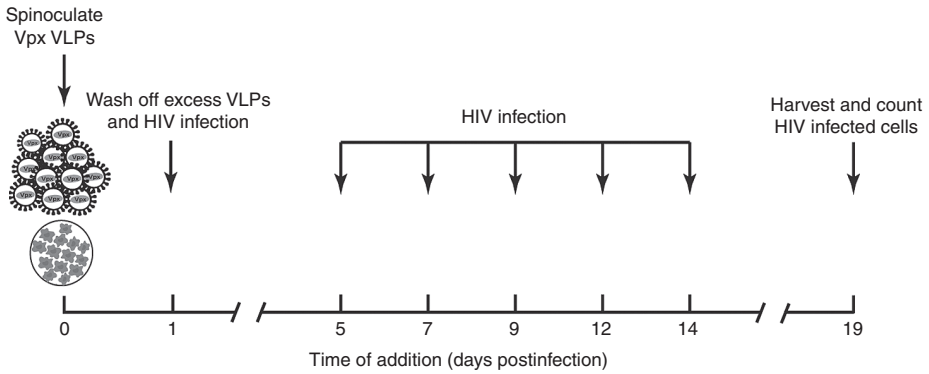

Figure 2 Protocol outline to determine the long term Vpx effect on HIV-1 infection.

results clearly demonstrate that the decreased efficacy of nucleoside reverse transcription inhibitor, AZT, and integrase inhibitor RAL persists for long-term.

Effectiveness of Vpx incorporation into LV gene therapy vectors is dependent on which part of HIV-1 replication is being targeted

To evaluate the therapeutic potential of incorporating Vpx with anti-HIV-1 genes we used two gene therapy strategies that inhibit HIV-1 replication at stages pre- and post-RT. This was primarily motivated by the influence Vpx has on RT in the short and long-term. The pre-RT approach inhibits viral entry, while the post-RT approach prevents post-transcriptional activity after viral integration occurs. The first approach utilizes a vector called Cal-1, which encodes a short hairpin RNA (shRNA) for the down-regulation of C-C chemokine receptor type 5 (CCR5) in combination with the HIV-1 fusion inhibitor, C46.[45] This construct has been used in nonhuman primates, a humanized mouse model and is currently undergoing phase 1/2 trials in the US.[46,47] The second approach uses a vector encoding an shRNA called shPromA, which targets the HIV-1 5′ long terminal repeats (LTR) promoter and induces profound silencing of integrated HIV-1. Studies have shown that shPromA suppresses viral replication long-term by epigenetic modifications through an RNAi pathway called transcriptional gene silencing .[22,48,49]

Despite dendritic cells showing a greater effect with Vpx, macrophages were selected to determine the effectiveness of these strategies in the presence of Vpx. The focus of our study was targeting the HIV-1 latent reservoir and macrophages have a more accepted role in contributing to the viral reservoir than dendritic cells.[50–54] The anti-HIV-1 genes therapy vectors were generated and packaged *in*

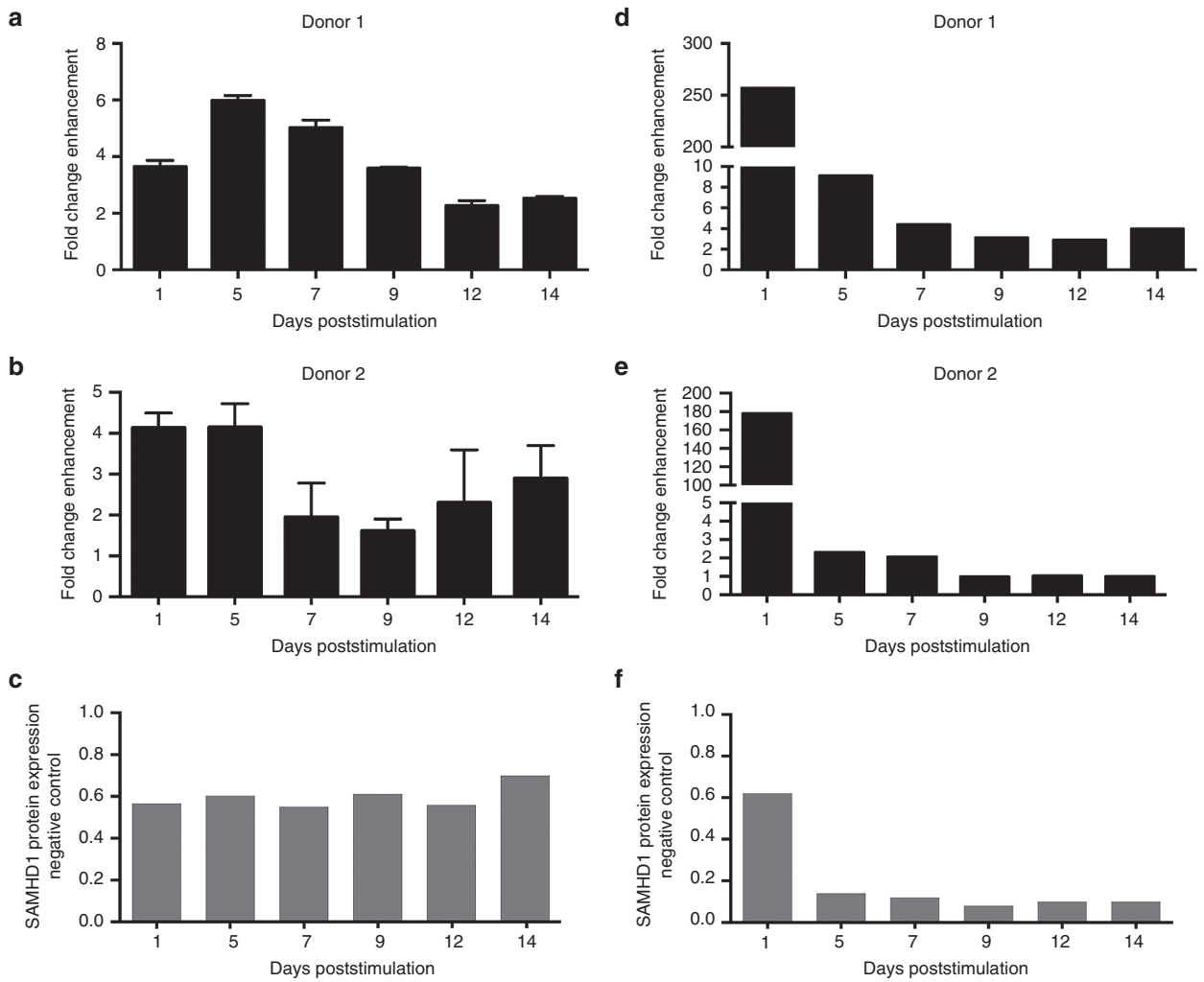

Figure 3 The long-term effect of Vpx on HIV-1 infection. (**a**,**b**, and **c**) Fold change enhancement of HIV-1 infection and SAMHD1 protein expression of Vpx stimulated macrophages up to 14 dps. Macrophages were spinoculated with Vpx VLPs and then challenged with HIV-1 at the indicated time points. Fold change enhancement was determined by enumerating GFP positive cells and normalizing the numbers to unstimulated cells. Two representative donors are shown. Protein expression of SAMHD1 was determined by western blot. Data was normalized to actin and represented as portion of the negative control. One representative MDM donor of three is displayed. (**d, e,** and **f**) Fold change enhancement of HIV-1 and SAMHD1 protein expression of Vpx stimulated MDDCs up to 14 dps. Two representative donors are shown the fold change enhancement and protein expression of SAMHD1 was analyzed as previously described in. GFP, green fluorescent protein; MDM, monocyte derived macrophage; MDDCs, monocyte derived dendritic cells; VLPs, virus-like particles.

trans with or without Vpx. Appropriate controls encoding GFP were also generated for both gene therapy approaches. All expression constructs encoded GFP, which acted as a reporter for successful transduction. A high content microscopy approach was used for the HIV-1 challenge experiments enabling individual cell analysis. Briefly, macrophages were transduced and at time points 7 and 14 days post-transduction (dpt) were challenged with infectious R5 BaL virus at increasing multiplicity of infections (MOIs). High throughput image acquisition was performed using the Cytell Cell Imaging System. Using Cell Investigator the total number of cells, transduced cells, and infected cells were enumerated. A linkage protocol was used to determine the number of transduced cells that were also infected. Distinguishing between transduced/uninfected cells and transduced/infected cells allowed us to determine the effectiveness of incorporating Vpx into gene therapy vectors.

At 14 dpt the transduction efficiencies for both Cal-1 and shPromA gene therapy approaches were significantly increased in the presence of Vpx, with fold changes of 85.4 ($P \leq 0.001$, $n = 3$) and 10.7 ($P \leq 0.01$, $n = 3$) observed for Cal-1 and Cal-1-eGFP and 9.0 ($P \leq 0.05$, $n = 3$) and 9.7 ($P \leq 0.05$, $n = 3$) for shPromA and shPromA-eGFP, respectively (Figure 5a,b). The gene transduction efficiencies observed at 7 dpt were also comparable (Supplementary Figure S4).

HIV-1 infection was analyzed in two measures, firstly, overall HIV-1 infection, which was independent of GFP transduction. Secondly, HIV-1 infection was specifically investigated in GFP transduced cells. At the highest MOI of 0.2, Cal-1 transduced cells showed the greatest inhibition in the presence of Vpx, with over a log reduction in HIV-1 infection compared to the –Vpx control (Figure 5c; Cal-1 (–Vpx) 2.64%, Cal-1 (+Vpx) 0.24%, $n = 3$). Only a small percentage of transduced cells were also infected, with 0.03 and 0.07% (Figure 5d $n = 3$) observed for Cal-1 (–Vpx) and Cal-1 (+Vpx) conditions, respectively. Indicating, in either the presence or absence of Vpx, Cal-1 transduced macrophages were protected against HIV-1 infection. No inhibition of HIV-1 infection was observed in the eGFP transduced cells, in the presence of Vpx, a 3.5-fold increase in HIV-1 infection was observed (Figure 5c; eGFP (–Vpx) 1.19%, eGFP (+Vpx) 4.15%; $n = 3$).

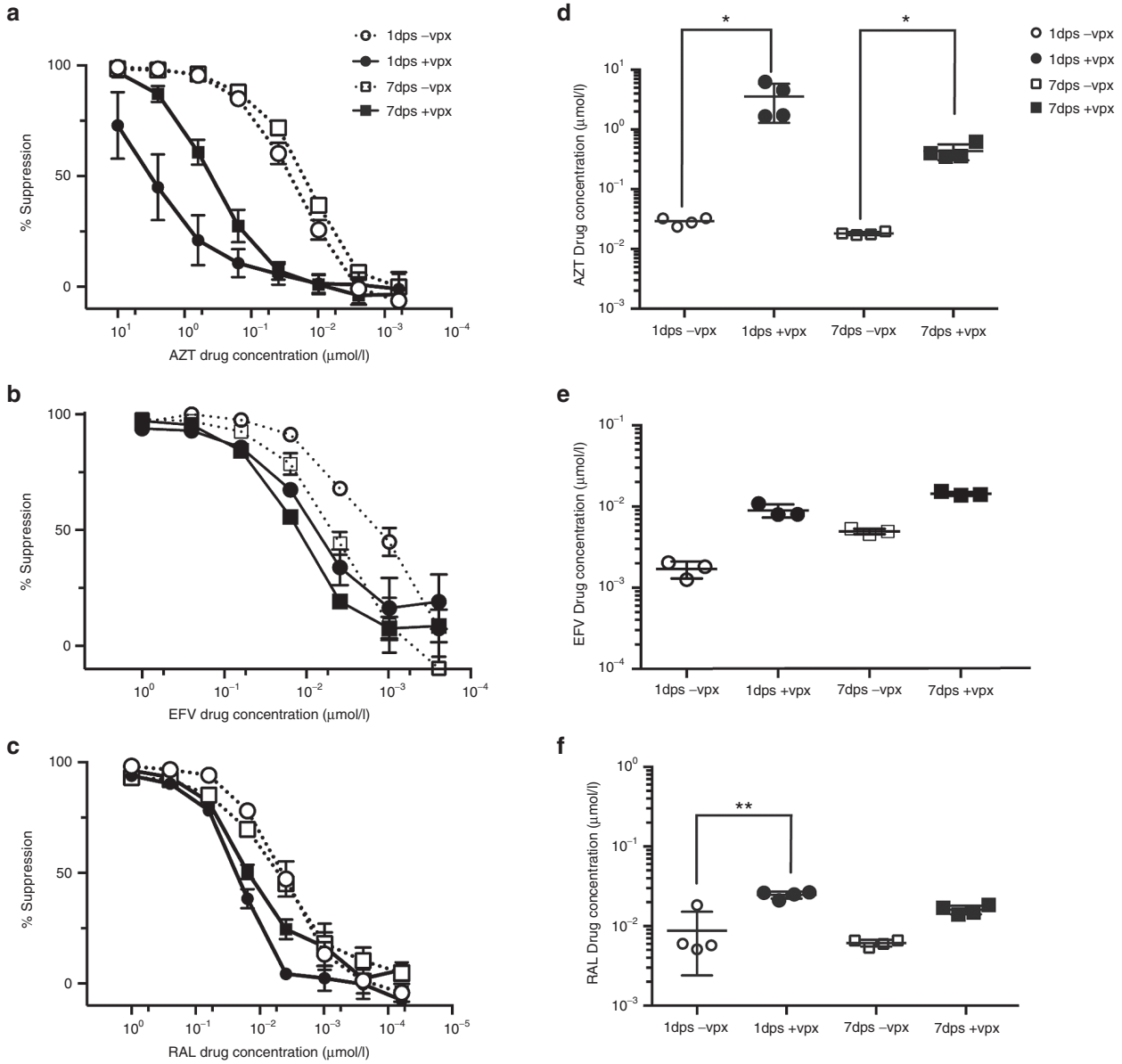

Figure 4 The long-term effect of Vpx on the efficiency of AZT, EFV, and RAL. Macrophages were stimulated with VLP packaged with or without Vpx for either 1 or 7 days before being treated with decreasing concentrations of AZT (**a**), EFV (**b**) or RAL (**c**) and infected with HIV-1 GFP. To determine the % of suppression, GFP positive cells were counted 5 days postinfection and normalized to nontreated cells stimulated with VLP ± Vpx. The IC_{50} values of AZT (**d**) were calculated using **a**, a nonparametric Kruskal–Wallis was used to determine the significance. The IC_{50} values of EFV (**e**) and RAL (**f**) were calculated using **b** and **c** respectively. The same statistical test was used as in **d**. Mean + SD were plotted; $n = 3$. One representative donor of three is displayed. AZT, azidothymidine; GFP, green fluorescent protein; SD, standard deviation; VLPs, virus-like particles.

Furthermore, HIV-1 infection of eGFP transduced cells increased by 40.3-fold in the presence of Vpx (Figure 5d; eGFP (–Vpx) 0.09%, eGFP (+Vpx) 3.63% $n = 3$). The above observations for eGFP-transduced cells were expected for two reasons; firstly, no anti-HIV-1 gene was encoded in the control plasmid. Secondly, in the presence of Vpx, successfully transduced cells would be primed for HIV-1 infection, therefore having a greater capacity for RT completion post-Vpx exposure. This was observed in both 7 and 14 dpt and across all MOI's 0.02, 0.1, and 0.2 (Supplementary Figure S5a–e). Additionally, there is no evidence of bystander cells demonstrating enhanced HIV-1 infection.

In the shPromA post-RT gene therapy condition, at the highest MOI of 0.2, we observed no inhibition of HIV-1 infection in the absence or presence of Vpx (Figure 5e; PromA (–Vpx) 1.14%, PromA (+Vpx) 2.72%, versus untransduced 0.61%; $n = 3$). In contrast, in the absence of Vpx at lower MOI's, protection against HIV-1 infection was observed (Supplementary Figure S6a–e). However, in the presence of Vpx, we also observed a 2.4-fold and 5.6-fold increase in HIV-1 infection for PromA and eGFP conditions, respectively (Figure 5e; $n = 3$). This trend was observed across all MOI's (Supplementary Figure S6a–e). HIV-1 infection in transduced cells also increased in the presence of Vpx by 20.1-fold and 36.2-fold for PromA and eGFP transduced conditions, respectively (Figure 5f). These observations were also present in time points 7 and 14 dpt and across HIV-1 challenges at increasing MOIs (Supplementary Figure S6a–e).

DISCUSSION

In this study, we have demonstrated that Vpx increases lentiviral RT and integration kinetics, which in turns increases levels of LV gene

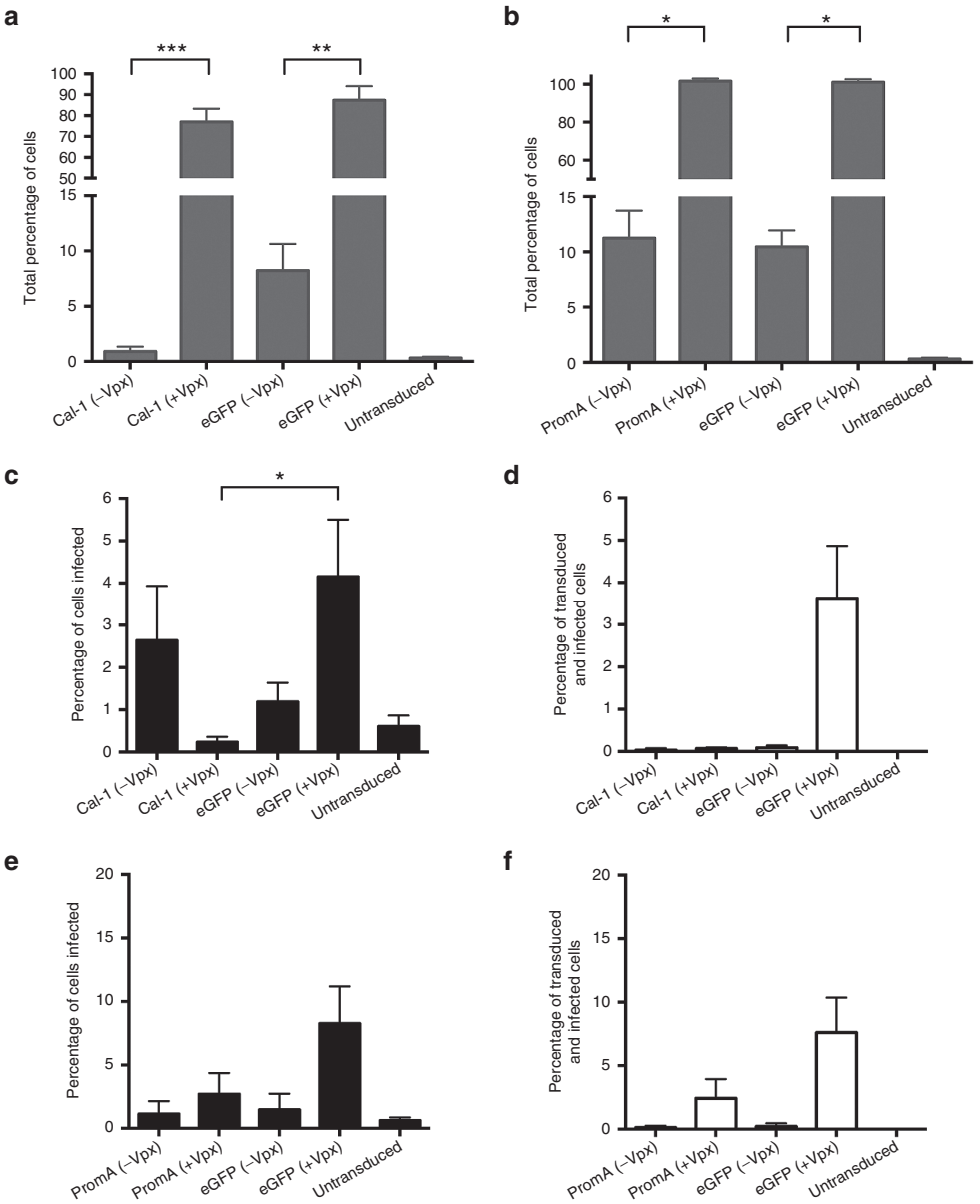

Figure 5 The effectiveness of Vpx incorporation into anti-HIV-1 gene therapy vectors. Macrophages were transduced with either Cal-1, PromA or their respective controls packaged with or without Vpx. At 14 dpt, the macrophages were infected with R5 BaL at MOI 0.2. After 7 days of infection, the cells were fixed and stained for p17/p24 and counterstained with DAPI. The cells were imaged on the Cytell and analysed using IN Cell Investigator software. Using DAPI as the denominator the percentage of transduced cells was calculated for Cal-1 (**a**) and shPromA (**b**), the percentage of infected cells for Cal-1 (**c**) and shPromA (**e**), and the percentage of transduced and infected cells for Cal-1 (**d**) and shPromA (**f**). The nonparametric Friedman test was used for statistical analyses. $P \leq 0.05$ (*), $P \leq 0.01$ (**) and $P \leq 0.001$ (***). Mean + SD were plotted; $n = 3$. One representative donor of three is displayed. DAPI, 4,6-diamidino-2-2-phenylindole; MOI, multiplicity of infection; SD, standard deviation.

delivery and transduction. The increased permissiveness persisted over a period of at least 2 weeks and consequently showed lowered potency to HIV-1 antiretrovirals that target HIV-1 RT or integration. This poses the possibility of detrimental complications if incorporating Vpx into LV gene therapy vectors for *in vivo/ex vivo* treatment of HIV-1 infected individuals. Since the cells reintroduced into the patient would be more permissive to HIV-1 infection, the treatment has the potential to increase the HIV-1 reservoir. The observed increase in IC_{50} values associated with Vpx treatment was of similar magnitude to prototypical resistant HIV-1 reverse transcriptase clones, such as HIV-1 4755-5 and 6463-13 (ref. 55). Furthermore, the decrease in AZT efficacy in the short-term is consistent with a previous study conducted by Amie and colleagues.[43,44] The increased IC_{50} observed post-Vpx treatment both short- and long-term in RAL treated cells was not equivalent to any prototypical resistant mutant strains.[56] Nonetheless, the decrease of AZT and RAL efficacy implies antiretroviral therapy may be influenced by Vpx exposure and thus either lead to reduced protection by therapy and/or promote subsequent viral replication and antiviral resistance.

While some of the previous observations are suggestive of the negative potential Vpx could have on the HIV-1 reservoir, the crucial test was investigating the effectiveness of anti-HIV-1 genes delivered with or without Vpx. To address this, two gene therapy approaches were used that inhibited HIV-1 infection either pre-RT (Cal-1) or post-RT (shPromA). The key step of HIV-1 replication that Vpx enhances is RT. Utilizing pre or post-RT approaches addressed

whether Vpx requires complementation with a specific category of anti-HIV-1 genes to effectively restrict HIV-1 infection. When Vpx was incorporated with the anti-HIV-1 genes, transduction efficiencies were significantly increased in both pre and post-RT approaches. In the absence of Vpx, both of the anti-HIV-1 gene approaches restricted HIV-1 infection. Furthermore, when examining on a single cell level, all transduced macrophages were protected against HIV-1 infection. However, in the presence of Vpx, the step at which the anti-HIV-1 gene restricted replication was critical in determining whether inhibition of HIV-1 replication occurred. Macrophages transduced with Cal-1, which restricts HIV-1 replication before RT at the step of entry/fusion, showed complete protection against HIV-1 infection in the presence of Vpx. However, macrophages transduced with shPromA, which restricts HIV-1 replication after RT, postintegration, failed to protect all of the macrophages with the majority of transduced cells also being infected with HIV-1. This effect observed for the post-RT approach was amplified when the MOI for HIV-1 infection increased. The reason for this lowered protective capacity could be due to an increase in viral RT-activity as a result of pre-Vpx exposure. An increase in viral RT and subsequent integration, could render shPromA unable to target all the HIV-1 genomes beyond a certain threshold level. Therefore, an increase in HIV-1 infection is observed when the MOI is increased. These results clearly demonstrate incorporating the Vpx protein with a pre-RT gene therapy approach significantly increases the number of successfully transduced resting cells, which in turn enhances HIV-1 protection levels. Furthermore, the use of Vpx does not have any deleterious bystander target effects as there is no evidence of nontransduced cells with an HIV-1 enhanced Vpx phenotype. *Ex vivo* gene delivery protocols need to wait till the protective anti-HIV-1 construct is active for reinfusion, as immediate transduction and then reinfusion into patients would render them highly permissive to HIV-1 infection.

The incorporation of Vpx protein into gene therapy vectors could also be beneficial in facilitating gene therapy protocols targeting resting cells, as there is an increase in both RT and integration kinetics upon Vpx stimulation alongside a significant increase in overall gene delivery. These effects could help in two key ways. Firstly, scaling up to generate Good Manufacturing Practice-compliant lentivirus batches for clinical trials would be economically more feasible. Since substantially less lentivirus would be required to achieve equivalent transduction rates a reduced number of batches for high-titer vector preparations would be needed. Typically, an MOI of at least 1 is used in clinical protocols, which is at least five times more than that used in our protocols.[45,47,57] Therefore the number of time consuming and rigorous tests required for each batch can be reduced. Additionally, using less lentivirus to achieve equivalent transduction rates would decrease the likelihood of toxicity, inflammation or immune responses observed *in vivo*.[58,59] Secondly, the time required to generate transduced cells for reinfusion could be decreased, since it takes significantly less amount of time to achieve successful gene expression due to the increase in RT and integration kinetics.

The long-term enhancement after Vpx stimulation observed in resting cells effectively restricts the use of this accessory protein to only pre-RT gene therapy approaches. To expand the use of Vpx, decreasing the window of opportunity to enhance lentiviral RT and integration kinetics needs to occur. One study has observed that Vpx is rapidly degraded in the cell through the proteasomal pathway.[41] Therefore, it could be hypothesized that the long-term phenotype is due to an interaction with a host protein. Indeed, our MDDC long term data showed the greatest enhancement of HIV-1 infection when SAMHD1 levels were at their highest. This interaction may not necessarily be SAMHD1, as a study by Hollenbaugh and colleagues has shown that post-Vpx treatment the rate of SAMHD1 recovery and dNTP depletion does not correlate.[60] Mutagenesis studies could reveal a novel mutant, which is unable to interact with the host protein responsible for the long-term phenotype, but retain the RT enhancing capacity of a short-term phenotype.

This study demonstrates a way to overcome the major delivery obstacle presented when delivering anti-HIV-1 genes into cells of the HIV-1 latent reservoir. Vpx significantly increased delivery with all gene therapy conditions. However, it was case-dependent whether the increase in gene delivery also translated into an enhanced antiviral effect, with Cal-1 pre-RT inhibition of HIV-1 replication showing the greatest effect. This result is of great importance, as Cal-1 is currently undergoing phase 1/2 trials in the United States. Additionally, oncology studies have started to incorporate Vpx in their gene therapy protocols.[61,62] For Vpx containing LV vectors, the dual utilization of Cal-1 (pre-RT), to protect against HIV-1 infection, and shPromA (post-RT), to stabilize the latent reservoir, would have the greatest effect on HIV-1 infected patients. For uninfected cells, the dual approach would prevent HIV-1 entry. For infected cells, the shPromA would restrict HIV-1 reactivation and Cal-1 would prevent any potential superinfection and enhancement of HIV-1 replication because of the presence of Vpx. The potential inclusion of Vpx in the future LV preparations may help further expand the delivery of this construct to unstimulated cells in clinical protocols, such as the resting CD4+ T cell population, as cells would not need to be stimulated/activated.

MATERIALS AND METHODS

Cells and cell culture

HEK293T cells (Invitrogen, Carlsbad, CA) and the HeLa cell line TZM-bl (Obtained through NIH AIDS Reagent Program, Division of AIDS, NIAID, NIH, from John C Kappes, Xiaoyun Wu and Tranzyme (Catalogue No. 8129)) were cultured in Dulbecco's modified Eagle's medium (DMEM) (Gibco, Waltham, MA) supplemented with 10% fetal calf serum (FCS) (Gibco).

Monocytes were purified from peripheral blood mononuclear cells by positive selection using anti-CD14 magnetic beads as outlined by the manufacturer (Miltenyi Biotech, Gladbach, Germany) with the exception of using phosphate-buffered saline (PBS) supplemented with 1% (v/v) human AB serum (Sigma Aldrich, St Louis, MO) and 1 mmol/l ethylenediaminetetraacetate (EDTA) (Sigma Aldrich) at 4°C. MDDCs were generated by culturing purified monocytes in Roswell Park Memorial Institute (RPMI) 1640 supplemented with 10% fetal calf serum (FCS), IL-4 (1,000 U/ml) and GM-CSF (1,000 U/ml) (Biosource, Carlsbad, CA) for 24 hours. MDMs were made by plastic adherence of monocytes in serum free media for 1 hour before supplemented with RPMI 1640 media containing human AB serum (Sigma Aldrich), which brought the final concentration of human serum to 10%. MDMs were used after 7 days of differentiation for experiments.

Plasmids

A second generation lentiviral vector capable of packaging Vpx was generated by subcloning the SphI-to-SbfI region containing the Vpx packaging motif from pNL4.3-luc3-E-R- SIV p6 17–26 (kind gift from N Landau) into psPAX2 (Obtained from Didier Trono through NIH AIDS Reagent Program, Division of AIDS, NIAID, NIH: psPAX2 (Catalogue No. 11348)) (see Supplementary Figure S1). The modified plasmid was termed psPvpxD. The HIV-1 GFP proviral clone (Δigag)[63] was used to generate HIV-GFP. The backbone is based on HIV-1 NL4.3 and contains eGFP in-between matrix and capsid, flanked 5′ and 3′ by HIV-1 protease cleavage sites. An early stop codon is also present in the *env* region. The lentiviral vectors shPromA and shPromA-empty were constructed as previously described.[64] The lentiviral vectors LVsh5/C46 (Cal-1) and Cal-1-empty were constructed as previously described.[45]

Virus preparations

VLPs packaged *in trans* in the presence or absence of Vpx, HIV-1 GFP and anti-HIV-1 lentiviral vectors were generated by cotransfecting HEK293T cells using linear PEI Max (at 1 mg/ml, pH 7 (Polysciences, PA)).

For the transfection of Vpx VLPs; psPvpxD, pMD2.G and pcVpx.myc (kindly provided by N Landau) or molecular grade salmon sperm DNA, was added at a DNA mass ratio of 2:1:0.7 respectively. Salmon sperm DNA served to maintain nitrogen to phosphate rations in PEI/DNA negative control transfections. The plasmids were diluted in tissue culture grade 0.9% (w/v) NaCl (Sigma Aldrich) into a final volume of 500 µl.

For the generation of HIV-1 GFP packaged with or without Vpx, the plasmids psPvpxD, Δigag,[63] pMD2.G and pcVpx.myc or molecular grade salmon sperm DNA were added at a DNA mass ratio of 2:2:1:0.7. The Δigag plasmid was cotransfected with psPvpxD for two reasons. Firstly to allow the packaging of Vpx into the virion and secondly for wild type (WT) Gag and WT Gag-Pol to be packaged into the assembling virions generating an unattenuated virus.

For the generation of shPromA and shPromA-eGFP packaged with or without Vpx, the plasmids psPvpxD, shPromA/shPromA-eGFP, pMD2.G and pcVpx.myc or molecular grade salmon sperm DNA were added at a DNA mass ratio of 2:2:1:0.7. For the generation of LVsh5/C46 (Cal-1) and Cal-1-eGFP[45] packaged with or without Vpx, the plasmids psPvpxD, Cal-1/Cal-1-eGFP, pMD2.G and pcVpx.myc or molecular grade salmon sperm DNA were added at a DNA mass ratio of 2:2:1:0.7.

As prepared above, 60 µl of polyethylenimine (PEI) Max (Polysciences, Warminster, PA) was added drop wise to the diluted plasmid DNA and vortexed for 10 seconds. The plasmid-DNA mix was incubated at room temperature for 30 minutes and then 7×10^6 trypsinised HEK293T cells were added dropwise to the mixture and incubated for 5 minutes at room temperature. This mixture was added dropwise to a 10 cm petri dish and the final volume was brought to 10 ml with DMEM supplemented with 10% FCS. The media was changed 18 hours after transfection with fresh media. At 72 hours post-transfection the supernatant was harvested by centrifugal preclearing of viral supernatant at 2,500×*g* for 20 minutes at 4°C, aliquoted and frozen at −80°C. For lentiviruses encoding anti-HIV-1 genes, the transfection supernatant was pelleted at 27,000×*g* for 90 minutes (no brake) after the initial preclear step and was resuspended in 20% RPMI.

Subsequently generated HIV-GFP and lentiviruses were titred on the indicator cell line TZMbl and the Reed Muench method was used to extrapolate the virus titre.[65] Since the VLPs ± Vpx do not produce the HIV-1 Tat protein to drive the reporter gene in the TZMbl indicator cell line, their titre was determined using reverse transcriptase activity as previously described.[66–68]

The R5 virus BaL was produced by transfecting HEK293T with the plasmid pWT/BaL (Obtained from Bryan R Cullen through NIH AIDS Reagent Program, Division of AIDS, NIAID, NIH: pWT/BaL (Catalogue No. 11414)). The resulting virus was then expanded using CCR5 positive Sup-T1 cell line (CL.30 courtesy of James Hoxie). The titre was obtained using the TZMbl indicator cell line, which was calculated to be 1.02×10^6/ml.

Immunoblot analysis

Whole cell lysates were generated using cell lysis buffer (Cell Signaling Technology, Danvers, MA) containing 20 mmol/l Tris-HCl (pH 7.5), 150 mmol/l NaCl, 1 mmol/l Na2EDTA, 1 mmol/l ethyleneglycol-bis(baminoethylether)- *N,N9*-tetraacetic acid (EGTA), 1% (v/v) Triton, 2.5 mmol/l sodium pyrophosphate, 1 mmol/l beta-glycerophosphate, 1 mmol/l Na_3VO_4, 1 µg/ml leupeptin with 1X complete mini protease inhibitor (Roche, Basel, Switzerland) added before use. The cells were incubated on ice for 30 minutes and vortexed every 10 minutes. The insoluble material was removed by centrifugation at 14,000×*g*, 4°C for 10 minutes. Supernatants were stored at −80°C before use.

Cell lysates were separated on 4–12% Bis-Tris sodium dodecyl sulfate (SDS)- polyacrylamide gel electrophoresis (PAGE) (Invitrogen) and transferred to a Polyvinylidene difluoride (PVDF) membrane (Millipore, Darmstadt, Germany). The membrane was blocked with 2.5% (w/v) skim milk in Tris-buffered saline (TBS) for 1 hour. The membrane was probed with either polyclonal antirabbit SAMHD1 antibody (611–625) (Sigma Aldrich) overnight at 4°C or anti-mouse β-actin (Monoclonal clone AC-15) (Sigma Aldrich) for 1 hour at room temperature. The membrane was washed (three times for 5 minutes with TBS-T) and probed with either donkey antirabbit IgG HRP or sheep antimouse IgG horseradish peroxidase (HRP) (GE Healthcare, Buckinghamshire, UK) for 2 hours at room temperature. The membrane was washed (three times for 5 minutes with TBS-T) and developed using Immun-Star HRP Chemiluminescent Kit (BioRad, Hercules, CA).

Flow cytometry

About 2.5×10^5 MDDCs were washed once in cold PBS and then fixed with 4% (v/v) PFA (Electron Microscopy Science, PA) for 20 minutes at 4°C in the dark. Cells were washed three times with cold PBS supplemented with 1% (v/v) human serum and 1 mmol/l EDTA. The MDDCs were gated on forward and side scatter and analyzed for fluorescein isothiocyanate (FITC) fluorescence with mock-infected cells as a negative control.

Time of addition assay

Macrophages seeded at 1×10^5/well in a 96-well plate were spinoculated with either HIV-GFP ± Vpx (MOI 0.1) or ±Vpx VLPs (670 pg RT) at 1,200 × *g* for 30 minutes at 4°C. At the indicated time-point post infection (hpi) either 10 µmol/l of AZT (Obtained from the NIH AIDS Reagent Program, Division of AIDS, NIAID, NIH (Catalog No. 3485)), or 1 µmol/l of RAL (Obtained through the NIH AIDS Reagent Program, Division of AIDS, NIAID, NIH: Raltegravir (Catalog No. 11680) from Merck & Company) or ± Vpx VLPs (670 pg RT) were added to the macrophage cultures. After 5 days of infection the plate was fixed with 4% PFA and GFP positive cells were counted on a fluorescent Elispot plate reader (AID Diagnostika, Strasburg, Germany). Results were either presented as total GFP positive cells or as a percentage of HIV-1 infection using the HIV-1 no drug control as the denominator.

IC_{50} of AZT and RAL

Macrophages seeded at 3.2×10^4/well in a 384 well plate were stimulated with ±Vpx VLPs (670 pg RT) for 1 and 7 days. At the stated time points, macrophages were treated with a fourfold dilution series of either AZT (starting concentration 10 µmol/l), EFV (starting concentration 1 µmol/l) or RAL (starting concentration 1 µmol/l) for 30 minutes before being spinoculated with HIV-1 GFP –Vpx (MOI = 0.1) at 1,200 × *g* for 30 minutes at 4°C. At five dpi GFP positive cells were counted on the Deltavision (Applied Precision). The results were represented as percent suppression compared with the no drug control.

High-throughput microscopy

Macrophages were seeded at 3.2×10^4/well in a 384 well plate and transduced at MOI 0.2 with anti-HIV-1 gene therapy vectors packaged with or without Vpx through spinoculation at 1,200 × *g* for 30 minutes at 4°C. At 7 or 14 days post-transduction the macrophages were infected with R5 BaL at three MOIs; 0.02, 0.1, and 0.2. At 7 dpi macrophages were fixed with 4% paraformaldehyde (PFA) (Sigma Aldrich) for 20 minutes at RT and then neutralized with 50 mmol/l NH4Cl (Sigma Aldrich) for 3 minutes. Cells were permeabilized with 0.05% Triton-X (Sigma Aldrich) for 1 minute at RT and blocked for 20 minutes in 10% goat serum. Macrophages were stained with the monoclonal antibodies p17 (ATCC; clone MH-SVM33C9) and p24 (Obtained from Bryan R Cullen through NIH AIDS Reagent Program, Division of AIDS, NIAID, NIH: pWT/BaL (Catalogue No. 11414[69]). The secondary antibody used was goat antimouse Alexa Fluor 647 (IgG H + L; Highly cross-absorbed; Invitrogen) All washes were performed in PBS supplemented with 1% fish skin gelatin (Sigma) and 0.02% saponin (Sigma Aldrich). The macrophages were counterstained with 4,6-diamidino-2-2-phenylindole (DAPI) (ThermoFisher, MA) before being visualized on the Cytell Cell Imaging System (GE Healthcare, Buckinghamshire, UK). The resulting images were transformed into a.XDCE file before being analysed by IN Cell Investigator software (GE Healthcare) to enumerate the total number of cells, transduced cells, and infected cells. A linkage protocol was used to determine the number of transduced cells that were also infected. A nonparametric analysis of variance (ANOVA) (Friedman test) was performed for all data sets along with a Dunn's multiple comparisons test.

CONFLICT OF INTEREST

The authors declare no conflict of interest.

ACKNOWLEDGMENTS

This work was supported by grants from the National Health and Medical Research Council 1052979 and 455350 for A.D.K., 630571 and 1049473 for K.S. and C.L.A., 1046703 and NHMRC Career Development Fellowship for S.G.T., C.A., A.D.K., K.S., and G.P.S. have patent applications for candidate siRNA sequences. S.G.T. and S.A.M. have a provisional patent application for Vpx use in gene therapy.

REFERENCES

1. Perelson, AS, Essunger, P, Cao, Y, Vesanen, M, Hurley, A, Saksela, K *et al.* (1997). Decay characteristics of HIV-1-infected compartments during combination therapy. *Nature* **387**: 188–191.
2. Perelson, AS, Essunger, P and Ho, DD (1997). Dynamics of HIV-1 and CD4+ lymphocytes *in vivo*. *AIDS* **11 Suppl A**: S17–S24.

3. Maldarelli, F, Palmer, S, King, MS, Wiegand, A, Polis, MA, Mican, J *et al.* (2007). ART suppresses plasma HIV-1 RNA to a stable set point predicted by pretherapy viremia. *PLoS Pathog* **3**: e46.
4. Chun, TW, Carruth, L, Finzi, D, Shen, X, DiGiuseppe, JA, Taylor, H *et al.* (1997). Quantification of latent tissue reservoirs and total body viral load in HIV-1 infection. *Nature* **387**: 183–188.
5. Finzi, D, Blankson, J, Siliciano, JD, Margolick, JB, Chadwick, K, Pierson, T *et al.* (1999). Latent infection of CD4+ T cells provides a mechanism for lifelong persistence of HIV-1, even in patients on effective combination therapy. *Nat Med* **5**: 512–517.
6. Wong, JK, Hezareh, M, Günthard, HF, Havlir, DV, Ignacio, CC, Spina, CA *et al.* (1997). Recovery of replication-competent HIV-1 despite prolonged suppression of plasma viremia. *Science* **278**: 1291–1295.
7. Sonza, S, Mutimer, HP, Oelrichs, R, Jardine, D, Harvey, K, Dunne, A *et al.* (2001). Monocytes harbour replication-competent, nonlatent HIV-1 in patients on highly active antiretroviral therapy. *AIDS* **15**: 17–22.
8. Harrigan, PR, Whaley, M and Montaner, JS (1999). Rate of HIV-1 RNA rebound upon stopping antiretroviral therapy. *AIDS* **13**: F59–F62.
9. Bloch, MT, Smith, DE, Quan, D, Kaldor, JM, Zaunders, JJ, Petoumenos, K *et al.* (2006). The role of hydroxyurea in enhancing the virologic control achieved through structured treatment interruption in primary HIV-1 infection: final results from a randomized clinical trial (Pulse). *J Acquir Immune Defic Syndr* **42**: 192–202.
10. Siliciano, JD, Kajdas, J, Finzi, D, Quinn, TC, Chadwick, K, Margolick, JB *et al.* (2003). Long-term follow-up studies confirm the stability of the latent reservoir for HIV-1 in resting CD4+ T cells. *Nat Med* **9**: 727–728.
11. Strain, MC, Gunthard, HF, Havlir, DV, Ignacio, CC, Smith, DM, Leigh-Brown, AJ *et al.* (2003). Heterogeneous clearance rates of long-lived lymphocytes infected with HIV: intrinsic stability predicts lifelong persistence. *Proc Nat Acad Sci USA* **100**: 4819–4824.
12. Murray, JM, Zaunders, JJ, McBride, KL, Xu, Y, Bailey, M, Suzuki, K *et al.*; PINT Study Team. (2014). HIV-1 DNA subspecies persist in both activated and resting memory CD4+ T cells during antiretroviral therapy. *J Virol* **88**: 3516–3526.
13. Perez, EE, Wang, J, Miller, JC, Jouvenot, Y, Kim, KA, Liu, O *et al.* (2008). Establishment of HIV-1 resistance in CD4+ T cells by genome editing using zinc-finger nucleases. *Nat Biotechnol* **26**: 808–816.
14. Holt, N, Wang, J, Kim, K, Friedman, G, Wang, X, Taupin, V *et al.* (2010). Human hematopoietic stem/progenitor cells modified by zinc-finger nucleases targeted to CCR5 control HIV-1 *in vivo*. *Nat Biotechnol* **28**: 839–847.
15. Cagnon, L and Rossi, JJ (2000). Downregulation of the CCR5 beta-chemokine receptor and inhibition of HIV-1 infection by stable VA1-ribozyme chimeric transcripts. *Antisense Nucleic Acid Drug Dev* **10**: 251–261.
16. Mitsuyasu, RT, Merigan, TC, Carr, A, Zack, JA, Winters, MA, Workman, C *et al.* (2009). Phase 2 gene therapy trial of an anti-HIV-1 ribozyme in autologous CD34+ cells. *Nat Med* **15**: 285–292.
17. An, DS, Donahue, RE, Kamata, M, Poon, B, Metzger, M, Mao, SH *et al.* (2007). Stable reduction of CCR5 by RNAi through hematopoietic stem cell transplant in non-human primates. *Proc Nat Acad Sci USA* **104**: 13110–13115.
18. Shimizu, S, Hong, P, Arumugam, B, Pokomo, L, Boyer, J, Koizumi, N *et al.* (2010). A highly efficient short hairpin RNA potently down-regulates CCR5 expression in systemic lymphoid organs in the hu-BLT mouse model. *Blood* **115**: 1534–1544.
19. Kim, SS, Peer, D, Kumar, P, Subramanya, S, Wu, H, Asthana, D *et al.* (2010). RNAi-mediated CCR5 silencing by LFA-1-targeted nanoparticles prevents HIV-1 infection in BLT mice. *Mol Ther* **18**: 370–376.
20. Liang, M, Kamata, M, Chen, KN, Pariente, N, An, DS and Chen, IS (2010). Inhibition of HIV-1 infection by a unique short hairpin RNA to chemokine receptor 5 delivered into macrophages through hematopoietic progenitor cell transduction. *J Gene Med* **12**: 255–265.
21. Weinberg, MS, Barichievy, S, Schaffer, L, Han, J and Morris, KV (2007). An RNA targeted to the HIV-1 LTR promoter modulates indiscriminate off-target gene activation. *Nucleic Acids Res* **35**: 7303–7312.
22. Suzuki, K, Ishida, T, Yamagishi, M, Ahlenstiel, C, Swaminathan, S, Marks, K *et al.* (2011). Transcriptional gene silencing of HIV-1 through promoter targeted RNA is highly specific. *RNA Biol* **8**: 1035–1046.
23. Lim, HG, Suzuki, K, Cooper, DA and Kelleher, AD (2008). Promoter-targeted siRNAs induce gene silencing of simian immunodeficiency virus (SIV) infection *in vitro*. *Mol Ther* **16**: 565–570.
24. Hollenbaugh, JA, Gee, P, Baker, J, Daly, MB, Amie, SM, Tate, J *et al.* (2013). Host factor SAMHD1 restricts DNA viruses in non-dividing myeloid cells. *PLoS Pathog* **9**: e1003481.
25. Hrecka, K, Hao, C, Gierszewska, M, Swanson, SK, Kesik-Brodacka, M, Srivastava, S *et al.* (2011). Vpx relieves inhibition of HIV-1 infection of macrophages mediated by the SAMHD1 protein. *Nature* **474**: 658–661.
26. Laguette, N, Sobhian, B, Casartelli, N, Ringeard, M, Chable-Bessia, C, Ségéral, E *et al.* (2011). SAMHD1 is the dendritic- and myeloid-cell-specific HIV-1 restriction factor counteracted by Vpx. *Nature* **474**: 654–657.
27. Goldstone, DC, Ennis-Adeniran, V, Hedden, JJ, Groom, HC, Rice, GI, Christodoulou, E *et al.* (2011). HIV-1 restriction factor SAMHD1 is a deoxynucleoside triphosphate triphosphohydrolase. *Nature* **480**: 379–382.
28. Lahouassa, H, Daddacha, W, Hofmann, H, Ayinde, D, Logue, EC, Dragin, L *et al.* (2012). SAMHD1 restricts the replication of human immunodeficiency virus type 1 by depleting the intracellular pool of deoxynucleoside triphosphates. *Nat Immunol* **13**: 223–228.
29. Beloglazova, N, Flick, R, Tchigvintsev, A, Brown, G, Popovic, A, Nocek, B *et al.* (2013). Nuclease activity of the human SAMHD1 protein implicated in the Aicardi-Goutieres syndrome and HIV-1 restriction. *J Biol Chem* **288**: 8101–8110.
30. Ryoo, J, Choi, J, Oh, C, Kim, S, Seo, M, Kim, SY *et al.* (2014). The ribonuclease activity of SAMHD1 is required for HIV-1 restriction. *Nat Med* **20**: 936–941.
31. Choi, J, Ryoo, J, Oh, C, Hwang, S and Ahn, K (2015). SAMHD1 specifically restricts retroviruses through its RNase activity. *Retrovirol* **12**: 46.
32. Lee, J and Zhou, P (2007). DCAFs, the missing link of the CUL4-DDB1 ubiquitin ligase. *Mol Cell* **26**: 775–780.
33. Srivastava, S, Swanson, SK, Manel, N, Florens, L, Washburn, MP and Skowronski, J (2008). Lentiviral Vpx accessory factor targets VprBP/DCAF1 substrate adaptor for cullin 4 E3 ubiquitin ligase to enable macrophage infection. *PLoS Pathog* **4**: e1000059.
34. Bergamaschi, A, Ayinde, D, David, A, Le Rouzic, E, Morel, M, Collin, G *et al.* (2009). The human immunodeficiency virus type 2 Vpx protein usurps the CUL4A-DDB1 DCAF1 ubiquitin ligase to overcome a postentry block in macrophage infection. *J Virol* **83**: 4854–4860.
35. Diamond, TL, Roshal, M, Jamburuthugoda, VK, Reynolds, HM, Merriam, AR, Lee, KY *et al.* (2004). Macrophage tropism of HIV-1 depends on efficient cellular dNTP utilization by reverse transcriptase. *J Biol Chem* **279**: 51545–51553.
36. Bobadilla, S, Sunseri, N and Landau, NR (2013). Efficient transduction of myeloid cells by an HIV-1-derived lentiviral vector that packages the Vpx accessory protein. *Gene Ther* **20**: 514–520.
37. Durand, S, Nguyen, XN, Turpin, J, Cordeil, S, Nazaret, N, Croze, S *et al.* (2013). Tailored HIV-1 vectors for genetic modification of primary human dendritic cells and monocytes. *J Virol* **87**: 234–242.
38. Geng, X, Doitsh, G, Yang, Z, Galloway, NL and Greene, WC (2014). Efficient delivery of lentiviral vectors into resting human CD4 T cells. *Gene Ther* **21**: 444–449.
39. Norton, TD, Miller, EA, Bhardwaj, N and Landau, NR (2015). Vpx-containing dendritic cell vaccine induces CTLs and reactivates latent HIV-1 *in vitro*. *Gene Ther* **22**: 227–236.
40. Daelemans, D, Pauwels, R, De Clercq, E and Pannecouque, C (2011). A time-of-drug addition approach to target identification of antiviral compounds. *Nat Protoc* **6**: 925–933.
41. Sunseri, N, O'Brien, M, Bhardwaj, N and Landau, NR (2011). Human immunodeficiency virus type 1 modified to package Simian immunodeficiency virus Vpx efficiently infects macrophages and dendritic cells. *J Virol* **85**: 6263–6274.
42. Naldini, L (2011). Ex vivo gene transfer and correction for cell-based therapies. *Nat Rev Genet* **12**: 301–315.
43. Amie, SM, Daly, MB, Noble, E, Schinazi, RF, Bambara, RA and Kim, B (2013). Anti-HIV-1 host factor SAMHD1 regulates viral sensitivity to nucleoside reverse transcriptase inhibitors via modulation of cellular deoxyribonucleoside triphosphate (dNTP) levels. *J Biol Chem* **288**: 20683–20691.
44. Hollenbaugh, JA, Schader, SM, Schinazi, RF and Kim, B (2015). Differential regulatory activities of viral protein X for anti-viral efficacy of nucleos(t)ide reverse transcriptase inhibitors in monocyte-derived macrophages and activated CD4(+) T cells. *Virol* **485**: 313–321.
45. Wolstein, O, Boyd, M, Millington, M, Impey, H, Boyer, J, Howe, A *et al.* (2014). Preclinical safety and efficacy of an anti-HIV-1 lentiviral vector containing a short hairpin RNA to CCR5 and the C46 fusion inhibitor. *Mol Ther Methods Clin Dev* **1**: 11.
46. Burke, BP, Levin, BR, Zhang, J, Sahakyan, A, Boyer, J, Carroll, MV *et al.* (2015). Engineering cellular resistance to HIV-1 infection *in vivo* using a dual therapeutic lentiviral vector. *Mol Ther Nucleic Acids* **4**: e236.
47. Peterson, CW, Haworth, KG, Burke, BP, Polacino, P, Norman, KK, Adair, JE *et al.* (2016). Multilineage polyclonal engraftment of Cal-1 gene-modified cells and *in vivo* selection after SHIV-1 infection in a nonhuman primate model of AIDS. *Mol Ther Methods Clin Dev* **3**: 16007.
48. Suzuki, K, Shijuuku, T, Fukamachi, T, Zaunders, J, Guillemin, G, Cooper, D *et al.* (2005). Prolonged transcriptional silencing and CpG methylation induced by siRNAs targeted to the HIV-1 promoter region. *J RNAi Gene Silencing* **1**: 66–78.
49. Yamagishi, M, Ishida, T, Miyake, A, Cooper, DA, Kelleher, AD, Suzuki, K *et al.* (2009). Retroviral delivery of promoter-targeted shRNA induces long-term silencing of HIV-1 transcription. *Microbes Infect* **11**: 500–508.
50. Igarashi, T., Brown, C. R., Endo, Y., Buckler-White, A., Plishka, R., Bischofberger, N *et al.* (2001). Macrophage are the principal reservoir and sustain high virus loads in rhesus macaques after the depletion of CD4+ T cells by a highly pathogenic simian immunodeficiency virus/HIV-1 type 1 chimera (SHIV): Implications for HIV-1 infections of humans. *Proc Nat Acad Sci USA* **98**: 658–663.
51. Kumar, A and Herbein, G (2014). The macrophage: a therapeutic target in HIV-1 infection. *Mol Cell Ther* **2**: 10.
52. Abbas, W, Tariq, M, Iqbal, M, Kumar, A and Herbein, G (2015). Eradication of HIV-1 from the macrophage reservoir: an uncertain goal? *Viruses* **7**: 1578–1598.

53. Honeycutt, JB, Wahl, A, Baker, C, Spagnuolo, RA, Foster, J, Zakharova, O *et al.* (2016). Macrophages sustain HIV-1 replication *in vivo* independently of T cells. *J Clin Invest* **126**: 1353–1366.
54. Margolis, DM, Garcia, JV, Hazuda, DJ and Haynes, BF (2016). Latency reversal and viral clearance to cure HIV-1. *Science* **353**: aaf6517.
55. Shafer, RW (2006). Rationale and uses of a public HIV-1 drug-resistance database. *J Infect Dis* **194 Suppl 1**: S51–S58.
56. Fransen, S, Gupta, S, Danovich, R, Hazuda, D, Miller, M, Witmer, M *et al.* (2009). Loss of raltegravir susceptibility by human immunodeficiency virus type 1 is conferred via multiple nonoverlapping genetic pathways. *J Virol* **83**: 11440–11446.
57. Uchida, N, Hsieh, MM, Hayakawa, J, Madison, C, Washington, KN and Tisdale, JF (2011). Optimal conditions for lentiviral transduction of engrafting human CD34+ cells. *Gene Ther* **18**: 1078–1086.
58. Baekelandt, V, Eggermont, K, Michiels, M, Nuttin, B and Debyser, Z (2003). Optimized lentiviral vector production and purification procedure prevents immune response after transduction of mouse brain. *Gene Ther* **10**: 1933–1940.
59. Geraerts, M, Michiels, M, Baekelandt, V, Debyser, Z and Gijsbers, R (2005). Upscaling of lentiviral vector production by tangential flow filtration. *J Gene Med* **7**: 1299–1310.
60. Hollenbaugh, JA, Tao, S, Lenzi, GM, Ryu, S, Kim, DH, Diaz-Griffero, F *et al.* (2014). dNTP pool modulation dynamics by SAMHD1 protein in monocyte-derived macrophages. *Retrovirol* **11**: 63.
61. Tareen, SU, Kelley-Clarke, B, Nicolai, CJ, Cassiano, LA, Nelson, LT, Slough, MM *et al.* (2014). Design of a novel integration-deficient lentivector technology that incorporates genetic and posttranslational elements to target human dendritic cells. *Mol Ther* **22**: 575–587.
62. Odegard, JM, Kelley-Clarke, B, Tareen, SU, Campbell, DJ, Flynn, PA, Nicolai, CJ *et al.* (2015). Virological and preclinical characterization of a dendritic cell targeting, integration-deficient lentiviral vector for cancer immunotherapy. *J Immunother* **38**: 41–53.
63. Aggarwal, A, Iemma, TL, Shih, I, Newsome, TP, McAllery, S, Cunningham, AL *et al.* (2012). Mobilization of HIV-1 spread by diaphanous 2 dependent filopodia in infected dendritic cells. *PLoS Pathog* **8**: e1002762.
64. Suzuki, K, Hattori, S, Marks, K, Ahlenstiel, C, Maeda, Y, Ishida, T *et al.* (2013). Promoter targeting shRNA suppresses HIV-1 infection *in vivo* through transcriptional gene silencing. *Mol Ther Nucleic Acids* **2**: e137.
65. Reed, LJ and Muench, H (1938). A simple method of estimating fifty per cent endpoints. *Am J Hygiene* **27**: 493–497.
66. Suzuki, K, Craddock, BP, Kano, T and Steigbigel, RT (1993). Chemiluminescent enzyme-linked immunoassay for reverse transcriptase, illustrated by detection of HIV-1 reverse transcriptase. *Anal Biochem* **210**: 277–281.
67. Suzuki, K, Craddock, BP, Okamoto, N, Kano, T and Steigbigel, RT (1993). Poly A-linked colorimetric microtiter plate assay for HIV-1 reverse transcriptase. *J Virol Methods* **44**: 189–198.
68. Suzuki, K, Saito, T, Kondo, M, Osanai, M, Watanabe, S, Kano, T *et al.* (1995). Poly A-linked non-isotopic microtiter plate reverse transcriptase assay for sensitive detection of clinical human immunodeficiency virus isolates. *J Virol Methods* **55**: 347–356.
69. Chesebro, B, Wehrly, K, Nishio, J and Perryman, S (1992). Macrophage-tropic human immunodeficiency virus isolates from different patients exhibit unusual V3 envelope sequence homogeneity in comparison with T-cell-tropic isolates: definition of critical amino acids involved in cell tropism. *J Virol* **66**: 6547–6554.

Supplementary Information accompanies this paper on the *Molecular Therapy—Methods & Clinical Development* website (http://www.nature.com/mtm)